The 9th International *Horticulture Research* Conference
Wuhan, Nov 2022

Integrative Analysis of Metabolome and Transcriptome Provides Insights into the Mechanisms of Anthocyanin Biosynthesis in Chinese Cherry (*Cerasus pseudocerasus* Lindl.) Fruit

Yan Wang[1,2,+], Zhiyi Wang[1,2,+], Jing Zhang[1,2,+], Hao Wang[1,2], Hongxia Tu[1,2], Jingting Zhou[1,2], Zhenshan Liu[1,2], Xirui Luo[1,2], Qing Chen[1], Wen He[1,2], Shaofeng Yang[1,2], Mengyao Li[1], Yuanxiu Lin[1,2], Yunting Zhang[1,2], Yong Zhang[1], Ya Luo[1], Haoru Tang[1,2], Xiaorong Wang[1,2,*]

[1]College of Horticulture, Sichuan Agricultural University, Chengdu 611130, Sichuan, P.R. China; [2]Institute of Pomology and Olericulture, Sichuan Agricultural University, Chengdu 611130, Sichuan, P.R. China.
[+]These authors contributed equally to this work. *Corresponding author: wangxr@sicau.edu.cn

ABSTRACT

Chinese cherry [*Cerasus pseudocerasus* (Lindl.) G.Don], native to China, has excellent nutritional, economic, and ornamental values with different fruit color. The red coloration of fruit is determined by anthocyanin pigmentation, which is an attractive trait for consumers. To date, the mechanisms underlying fruit color formation in Chinese cherry fruit have not been reported yet. In this study, the pigmentation patterns in (dark)-red and yellow fruit of Chinese cherry were illustrated by integrated widely-targeted metabolome and transcriptome analyses. Anthocyanin content and color ratio (a^*/b^*) in (dark)-red fruit was significantly higher compared with yellow fruit at mature stage. Metabolomic profiling revealed that cyanidin-3-*O*-rutinoside was the predominant anthocyanin compound in both fruit, while it was 6.23-fold higher in dark-red than in yellow fruit. Pelagonidin-3-*O*-rutinoside, pelargonidin-3-*O*-glucoside, peonidin-3-*O*-glucoside, and pelargonidin-3-*O*-glucoside-5-*O*-arabinoside were present only in dark-red fruit, also being responsible for the dark-red peel color. In addition, more accumulated procyanidins, flavanols, and isoflavones might result in less anthocyanins in flavonoid pathway for yellow fruit. Through comparative transcriptomics and weighted gene co-expression network analysis, ten genes were identified to be involved in anthocyanin biosynthesis and transport pathway, including seven biosynthesis genes (*CpCHS*, *CpCHI*, *CpF3H*, *CpF3'H*, *CpDFR*, *CpANS*, *CpUFGT*), one transport gene (*CpGST*), and two transcription factors (MYB10, IBH1). Transcriptome data and real-time PCR showed that the transcript levels of these genes were significantly higher in dark-red fruit than in yellow fruit at later stage, especially *CpANS*, *CpUFGT*, and *CpGST*, suggesting they may play important roles in red-colored fruit formation. *CpLAR* was higher in yellow fruit than dark-red fruit, especially at the early stage, which promoted the accumulation of flavanols and procyanidins in yellow fruit. These results provide novel insights into color patterns formation mechanisms of Chinese cherry fruit, and the candidate key genes identified in anthocyanin biosynthesis may provide a valuable resource for Chinese cherry breeding program in the future.

Physiological Indices in Red and Yellow Fruits of Chinese cherry

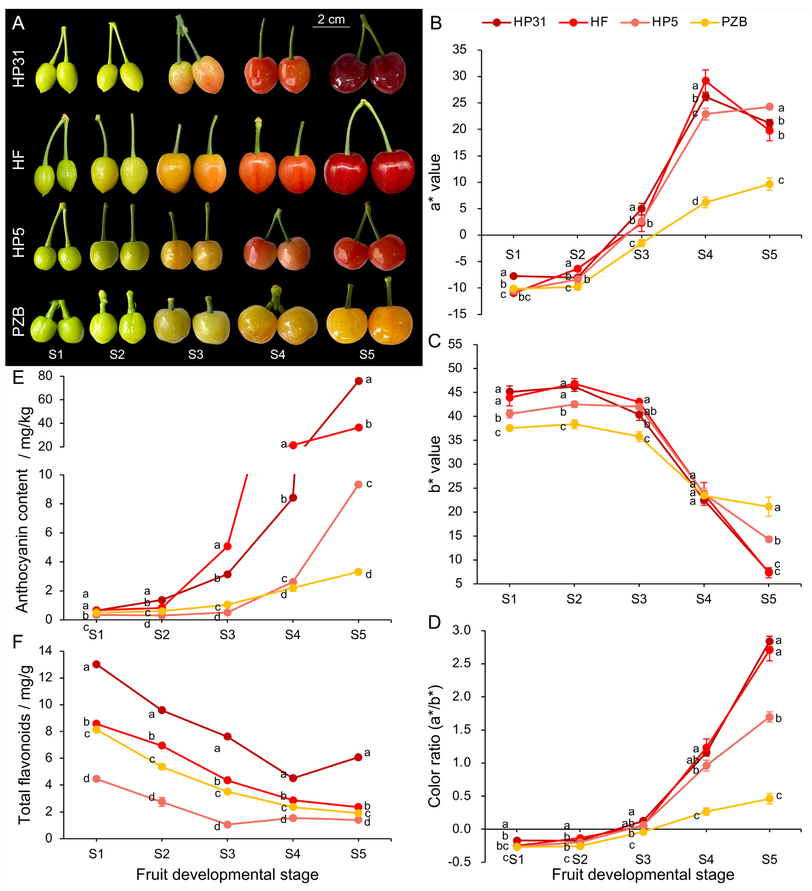

Fig. 1 Phenotypes and physiological changes of (dark)-red and yellow fruits of Chinese cherry during fruit development: (**A**) Fruit phenotypes. (**B**) Changes in a^* values. (**C**) Changes in b^* values. (**D**) Changes in a^*/b^* color ratio. (**E**) Changes in total anthocyanin content. (**F**) Changes in total flavonoids content. The a^* coordinate represents the red (positive)-to-green (negative) scale, and the b^* coordinate represents the yellow (positive)-to-blue (negative) scale. Error bars represent ± SD from three independent replicates. The lower case letter indicate significant difference at 0.05 level.

Comparison of Metabolites Between Dark-red and Yellow Fruits

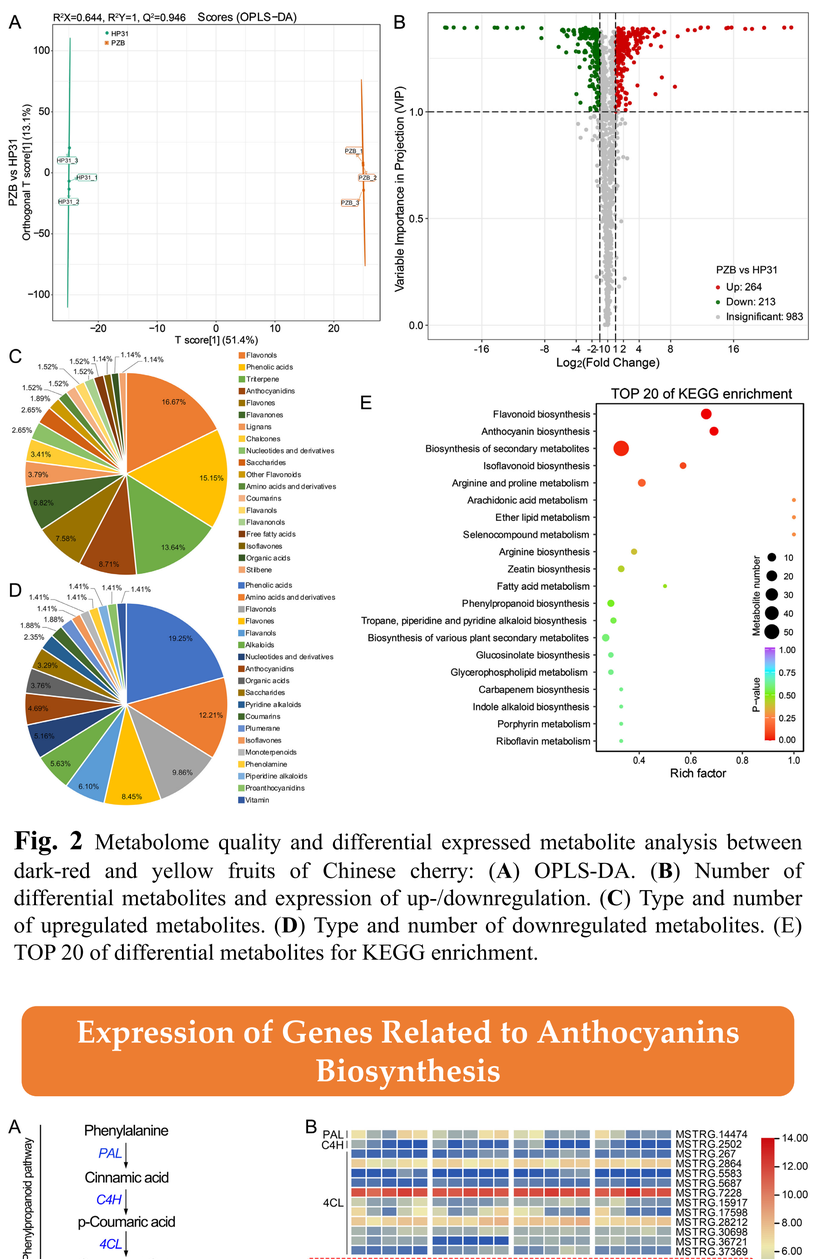

Fig. 2 Metabolome quality and differential expressed metabolite analysis between dark-red and yellow fruits of Chinese cherry: (**A**) OPLS-DA. (**B**) Number of differential metabolites and expression of up-/downregulation. (**C**) Type and number of upregulated metabolites. (**D**) Type and number of downregulated metabolites. (E) TOP 20 of differential metabolites for KEGG enrichment.

Identification and Comparison of Anthocyanin and Procyanidin Compounds

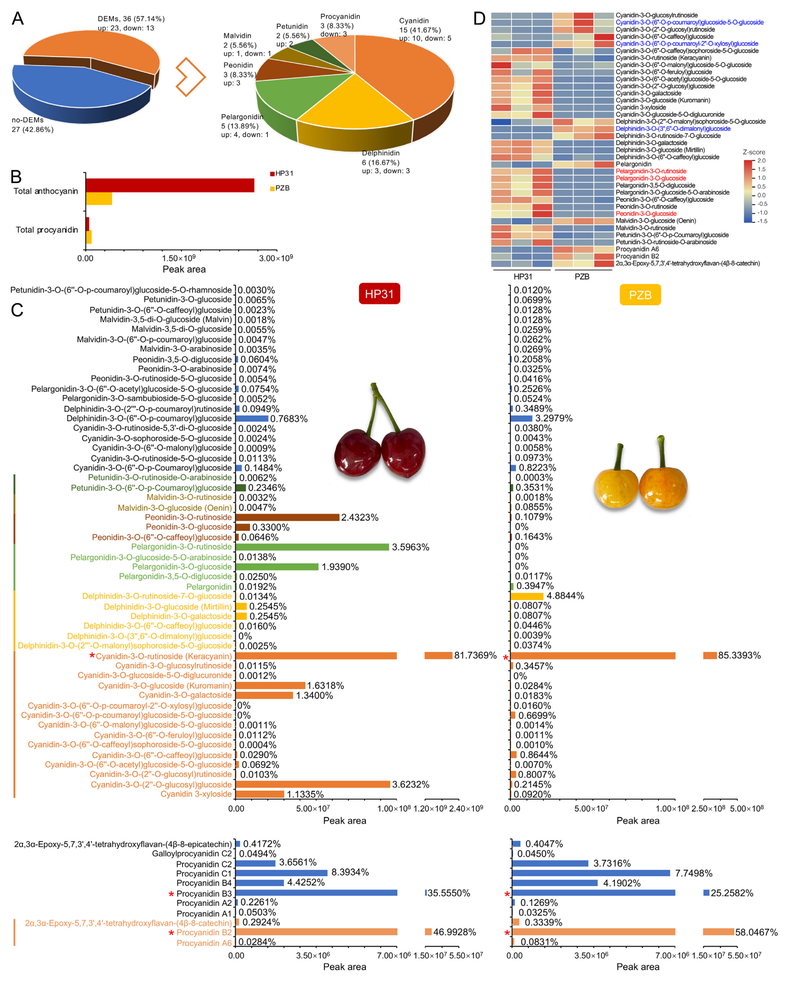

Fig. 3 Comparison of anthocyanin and procyanidin compounds between dark-red and yellow fruits of Chinese cherry: (**A**) Statistics of the expressed metabolites and differentially expressed metabolites. (**B**) The relative contents of total anthocyanin and total procyanidin from metabolome data. The relative content of metabolites is expressed by peak area. (**C**) The relative contents and proportion of anthocyanin (upper) and procyanidin (lower) compounds in red and yellow fruits of Chinese cherry. The colorful font indicates the 36 DEMs. Red asterisk indicates the major compounds. (**D**) Heatmap of the 36 DEMs at mature stage. Color indicates the relative content of each DEM, from blue (low) to red (high). Red and blue font indicates the top three up-regulated and down-regulated anthocyanins/procyanidins in the yellow vs. dark-red comparison.

Weight Gene Co-expression Network Analysis Based on Transcriptome Data

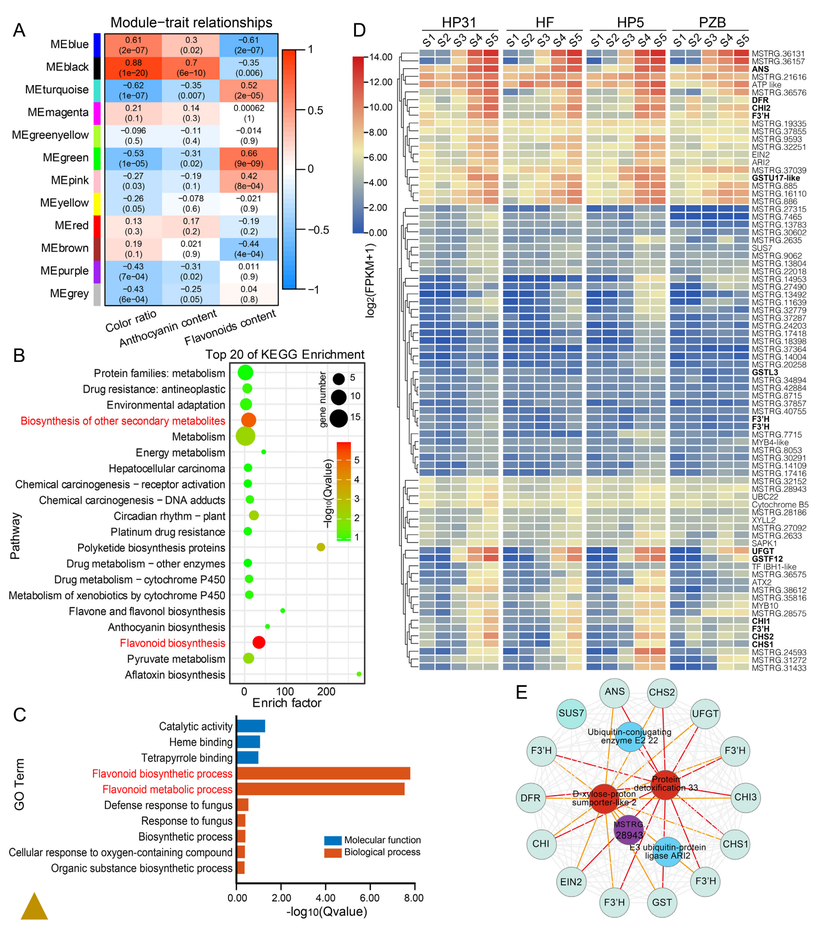

Fig. 4 WGCNA identified gene networks and key candidate genes involved in anthocyanin biosynthesis during fruit development of Chinese cherry: (**A**) Module-trait relationships based on Pearson correlations. The color key from blue to red represents r^2 values from -1 to 1. (**B**) KEGG enrichment analysis of with the top 20 KEGG pathways in the genes in the black module. (**C**) GO enrichment analysis of genes in the black module. (**D**) Heatmap of the expression level of genes in the black module. (**E**) Genes whose expression was highly correlated in the black module.

Expression of Genes Related to Anthocyanins Biosynthesis

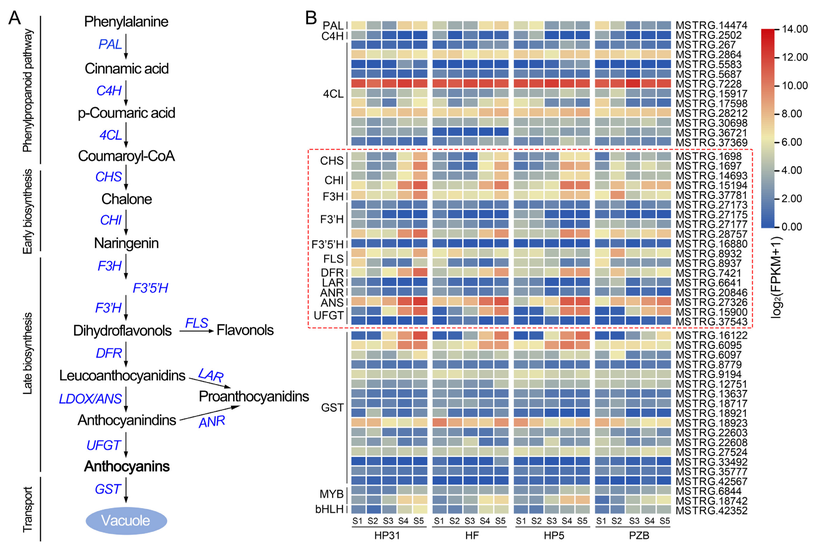

Fig. 5 The flavonoid biosynthetic pathway associated with anthocyanin biosynthesis in Chinese cherry fruit: (**A**) Simplified model of the anthocyanin biosynthesis pathway in Chinese cherry. (**B**) Anthocyanin biosynthesis pathway with related genes present in (dark)-red and yellow fruits of Chinese cherry.

A Hypothesis Model

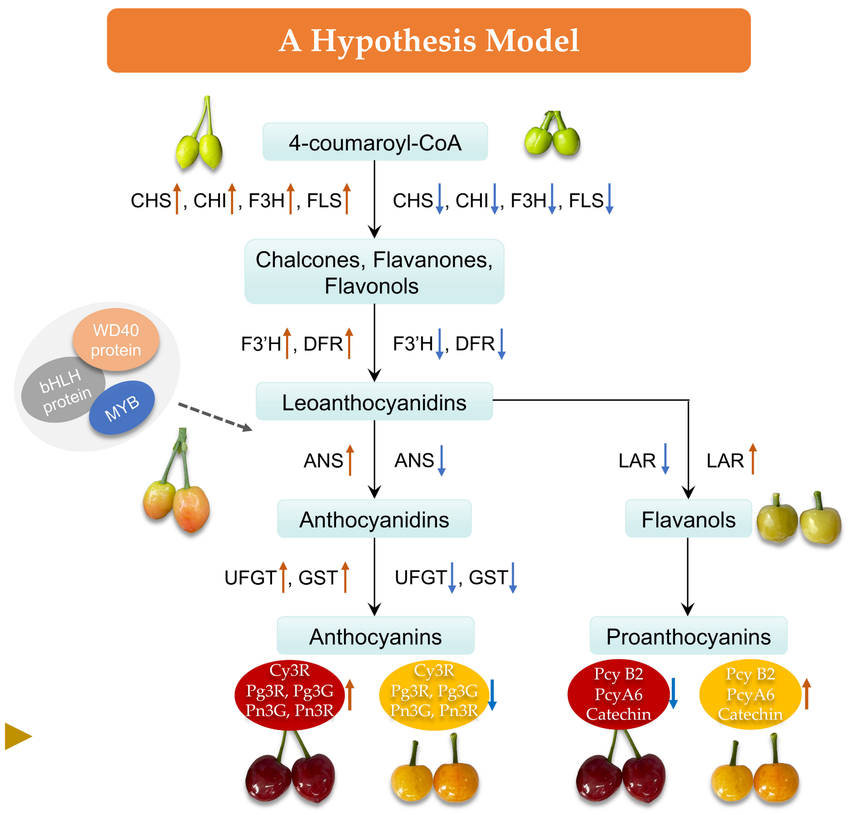

Fig. 7 A hypothesis model of gene expression regulating anthocyanin biosynthesis in dark-red and yellow Chinese cherry fruit. Changes of the gene expression and metabolites involved flavonoid biosynthesis pathway were listed. The arrow on the left and right represents 'HP31' and 'PZB'. The red and blue arrow represent the up-regulated and down-regulated flavonoids compounds or related-genes respectively. The black dotted lines indicate that the direct correlation was uncertain. Cy3R: cyanidin-3-*O*-rutinosice; Pg3R: pelargonidin-3-*O*-rutinoside; Pg3G: pelargonidin-3-*O*-glucoside; Pn3G: peonidin-3-*O*-glucoside; Pn3R: peonidin-3-*O*-rutinoside; Pcy: procyanidin.

Gene Expression Validation by qRT-PCR Analysis

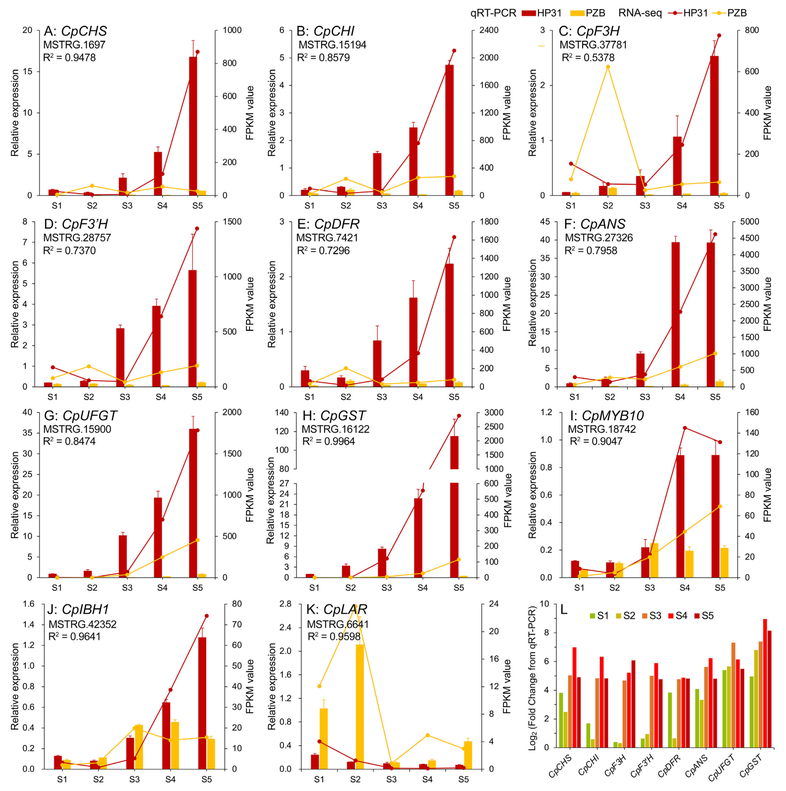

Fig. 6 Expression profiles of candidate genes related to the anthocyanin accumulation in Chinese cherry during fruit development: (**A-K**) Gene expression of key candidate genes involved in anthocyanin biosynthesis and transport. (**L**) Log_2Fold Change of differentially expressed anthocyanin-related genes between dark-red and yellow fruits from qRT-PCR.

ACKNOWLEDGEMENTS

This work was supported by Cherry Resources Sharing and Service Platform of Sichuan Province, Chengdu Technological Innovation Research and Development Project (Grant 2022YF05-01017-SN), Tianfu Talent Project of Chengdu City (Grant 2021-CF02-0162396-RC-4096), The Project of Rural Revitalization Research Institute in Tianfu New Area of Sichuan Province (Grant XZY1-04), Undergraduate Innovation Training Program in Sichuan Agricultural University (Grant S202210626089), and Shuangzhi Project Innovation Team of Sichuan Agricultural University (Grant P202107).